International Journal of Applied Engineering Research ISSN 0973-4562 Volume 12, Number 21 (2017) pp. 11523-11531

An Innovative Quality System for Surface Blemish Detection of Touch Panels

Hong-Dar Lin*, Jen-Miao Li,

Department of Industrial Engineering & Management, Chaoyang University of Technology, 168 Jifong E. Rd., Wufong District, Taichung, 41349, Taiwan.

**Orcid ID: 0000-0003-1875-8779*

Abstract

Touch panels are widely used in various electronic appliances such as smartphones, tablets, etc.. Difficulties exist in inspecting blemishes inlaid in appearances of panels with structural patterns. Area blemishes are a type of common appearance defect that includes dirt, water marks, bubbles, and other flaws of larger sizes. Such blemishes have the properties of low contrast, brightness with gradual changes, irregular and non-directional shapes, and occasionally both bright and dark blemishes co-existing in a region. This study proposes a wavelet transform-based approach to inspect the area blemishes on appearances of TPs. The Haar wavelet transform with flat zone filtering technique is applied to remove the structural patterns of background through filtering an approximated sub-image of a decomposed image in wavelet domain. Then, the filtered image is transformed back to spatial domain. Finally, the reconstructed image can be easily segmented into three categories (dark blemishes, bright blemishes, and background) by using a statistical interval estimation method. Therefore, the intricate area blemishes are precisely identified by the proposed scheme. Experimental results show that the developed inspection system achieves a high flaw detection rate of 90.68% and a low false alarm rate of 5.53%, and a high correct classification rate of 93.42%.

Keywords: Quality system, surface blemish detection, touch panels, wavelet transform.

INTRODUCTION

With the development of smartphones, general touchtone phones are gradually being replaced in order to stimulate a wave of touch screen devices. Touch panels (TPs) are adopted not only for mobile phones but also for computers, televisions, cameras, handheld game consoles and other 3C products; the increasing demand for touch panels promotes the development of the industry. Currently touch technology of screen panels can be primarily divided into resistive (an earlier technology), capacitive, optical, electromagnetic, and ultrasonic types. Since Resistive Touch Panels (RTPs) are susceptible to scrape and fire, low light transmittance, and slow response shortcomings, the RTP products cannot meet the modern requirements for touch technology and thus have a market share much lower than that of the Capacitive Touch Panels (CTPs). The CTPs, being an unshakable market leader in the touch panels industry, have the advantages of waterproofness, stain-proofness, scratch-proofness, fast response, anti-UV, etc.

Inspection of appearance blemishes on TPs has become an important task for manufacturers who try hard to improve the product quality and production efficiency of touch panels. The TPs are composed of transparent glass substrates, on the surface of which an oxide metal is regularly coated. Figure 1 shows a TP screen with repeated pattern structure of sensing circuits and an enlargement of part of a TP surface. The surfaces of TPs are multi-layer structured and are classified as structural textures. Appearance blemishes affect not only the surfaces of TPs but also their functionality, efficiency and stability. It is a difficult inspection task when flaws are inlaid in appearances of TPs with structural textures. Small appearance blemishes, frequently occurring in the manufacturing process of touch panels, cause much greater harms and impact when they appear in high-tech products than in industrial parts. Therefore, to survive in today's competitive market of high-tech products, touch panel producers cannot afford to neglect small appearance blemishes.

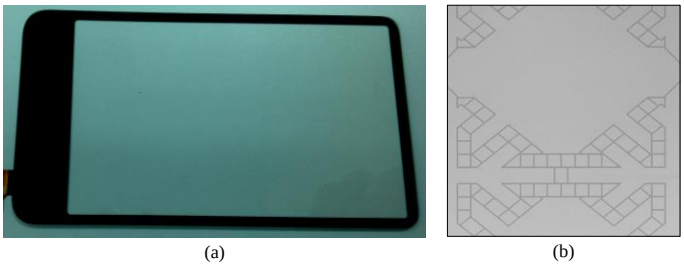

(a) (b)

Figure 1: A TP screen with repeated pattern structure of sensing circuits and an enlargement of part of a TP surface.

The appearance blemishes are usually classified into two types: linear and areal. The areal type includes dirt, water marks, bubbles and other flaws of larger sizes. Such blemishes have the properties of low contrast, brightness with gradual changes, irregular and non-directional shapes, and both bright and dark blemishes co-existing in a region. This kind of blemishes compared with the linear type is more complicate to identify its regularity. Thus, this study proposes an automatic detection system to inspect the areal blemishes on touch panels. Figure 2 shows two defective images of TP appearances with various area blemishes. The directional textures reveal lattice shapes with lines in four directions (horizontal, vertical, and two diagonals). These background textures make the flaw inspection task more difficult when area blemishes are inlaid in the appearances of directional textures. We accordingly propose an image restoration approach based on wavelet transform to overcome the difficulties of automatic areal flaw inspection of touch panels.

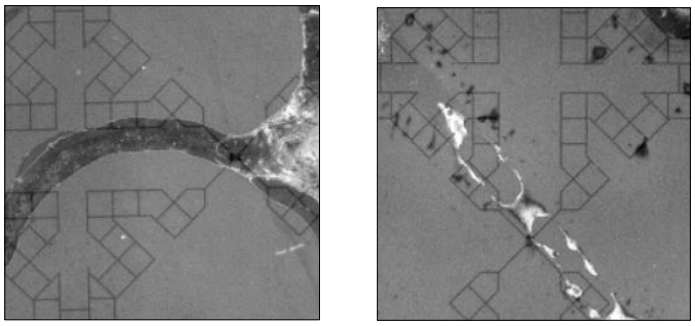

(a) (b)

Figure 2: Two defective TP images with various area blemishes.

Automatic inspection of appearance flaws has become an important work for industries who exert to enhance product quality and production efficiency [1-4]. Flaw inspection techniques compute a set of textural characteristics in a moving window and seek for crucial local changes among the feature vectors in the spatial domain or the frequency domain [5]. Kuo and Su [6] applied the co-occurrence matrix to extract fabric characteristics and the gray relational analysis to investigate the correlation of the analyzed factors among the selected characteristics for fabric defect classification. Yoon et al. [7] used image segmentation techniques to find defects from polarized film images and template matching techniques to determine defect types through the image analysis of detected defects. Yuan and Kuo [8] used model-based clustering algorithms via Bayesian inferences for flaw pattern detections, such as curvilinear patterns, ellipsoidal patterns and non-uniform global defect patterns, on semiconductor wafers.

Automatic thresholding has also been widely used in the computer vision applications for automatic optical inspection of blemishes [9]. The Otsu method [10] is one of the better threshold selection methods for general real world images with respect to uniformity and shape measures. This method chooses threshold values that maximize the between-class variances of the histogram. It provides satisfactory results for thresholding an image with a histogram of bimodal distribution. Ng [11] revised the Otsu method for selecting optimal threshold values for both unimodal and bimodal distributions, and tested the performance of the revised method on common flaw detection applications. Recently, Navarro et al. [12] presented a sensor system based on thresholding techniques for detecting flaws in ship hull appearances.

Fourier transform, wavelet transform and Gabor transform are common texture analysis techniques used in the frequency domain [13]. Nasira and Banumathi [14] used the Fourier transform and image processing to inspect fabric defects. Tsai and Hsiao [15] proposed a wavelet transform based approach for inspecting local flaws inlaid in homogeneous textured appearances. Lin [16] developed a wavelet-based multivariate statistical approach to automatically inspect ripple flaws with low intensity contrast in the appearance barrier layer chips of ceramic capacitors. Li [17] applied the wavelet transform to enhance defect regions and extract discriminative features from restored images and the support vector machine to classify five main defect categories on the copper clad laminate surfaces. Chang [18] addressed on structure design and implementation of real-time fabric defect detection system based on Gabor filtering. Lin and Chiu [19] combined block discrete cosine transform and grey relational analysis technique to inspect flaws on domed appearances in packages of light emitting diodes.

Directional textures have homogeneous patterns and are commonly found on man-made objects, such as machined parts, fabric textiles, and electronic components [20-21]. Lu and Tsai [22] presented a machine vision system based on an image reconstruction scheme using independent component analysis for automatic detection of micro blemishes in patterned TFT-LCD panel appearances that involve both simple and complicated patterns. Perng and Chen [23] developed a nonnegative matrix factorization based approach for automatically inspecting the flaws in directional texture appearances. As to inspecting blemishes of touch panels, Chen et al. [24] introduced an automatic optical inspection system for analogical RTP. This system integrates mechanism, electrical control and machine vision, and applies digital image processing method to inspect flaw of the RTP. The RTP has the texture of periodic spacers in spatial domain image and results in periodic dots in Fourier spectrum. Lin and Tsai [25] proposed a Fourier transform based approach to detect linear blemishes on CTP appearances. The linear blemishes such as scratches and cracks are regular blemishes with directional shapes. This kind of blemishes compared with the areal type is less complicated to identify its regularity.

MATERIALS AND METHODS

Problem Description

In this research, we explore the area flaw inspection of the popular TP products. When a TP image with four different directions of periodic lines in background texture is transformed to wavelet domain, the directional textures of background will be removed through filtering the approximated sub-image of a decomposed image in wavelet domain. It is difficult to precisely detect area blemishes inlaid in the complicated directional textures. Therefore, we present a global image restoration scheme using the wavelet transform and flat zone filtering process for area flaw detection on TP images. This scheme does not proceed with the processes of feature extraction and template matching.

This research proposes a wavelet based flat zone filtering approach to inspect area blemishes of touch panels. When a touch panel image with four different directional line patterns of sensing circuits is transformed to wavelet domain, the directional textures of background can be removed through filtering the approximated sub-image of the next decomposition level of Wavelet transform. The filtering scope is determined by a statistical interval. Within the range, the frequency components will be replaced by the mean value. Then, the filtered image is transformed back to spatial domain. Finally, the reconstructed image with enhanced blemishes can be easily segmented into three categories, dark blemishes, bright blemishes, and background, by using a simple statistical histogram method and some features of the detected blemishes are extracted.

PROPOSED METHOD

Wavelet Transform

Wavelet transform provides a convenient way to obtain a multi-resolution representation, from which texture features can be easily extracted. We use the Haar wavelet transform to conduct image transformation for frequency filtering, because the merits of Haar wavelet transform include local image processing, simple calculations, high speed processing, memory efficiency, and multiple image information [26-29]. The Haar wavelet transform is one of the simplest and basic wavelet transformations. A standard decomposition of a two-dimensional image can be done by first applying the 1-D Haar wavelet transform to each row of pixel values, treating these transformed rows as if they were themselves an image, and then performing another 1-D wavelet transform to each column. The Haar transform can be computed stepwise by the mean value and half of the differences of the tristimulus values of two contiguous pixels. Based on the transfer concept of the 1-D space, the Haar wavelet transform can process a 2-D image of (M x N) pixels in the following way:

Row transfer :

$$\begin{cases} f_R(i,j)=\left[\dfrac{f(i,2j)+f(i,2j+1)}{2}\right], \\ f_R(i,j+\left[\dfrac{N}{2}\right])=\left[\dfrac{f(i,2j)-f(i,2j+1)}{2}\right], \\ where\ 0\le i\le (M-1),\ 0\le j\le \left[\dfrac{N}{2}\right]-1,\ [\ ]\ is\ Gauss\ symbol. \end{cases}$$

Column transfer :

$$\begin{cases} f_C(i,j)=\left[\dfrac{f_R(2i,j)+f_R(2i+1,j)}{2}\right], \\ f_C(i+\left[\dfrac{M}{2}\right],j)=\left[\dfrac{f_R(2i,j)-f_R(2i+1,j)}{2}\right], \\ where\ 0\le i\le \left[\dfrac{M}{2}\right]-1,\ 0\le j\le (N-1). \end{cases} \quad (1)$$

In the above expressions (Eq. (1)), $f(i,j)$ represents an original image, $f_R(i,j)$ the row transfer function of $f(i,j)$, and $f_C(i,j)$ the column transfer function of $f_R(i,j)$. As $f_C(i,j)$ is also the outcome of the wavelet decomposition of $f(i,j)$, the outcomes of a wavelet transform can be defined as:

$$\begin{cases} A(i,j)=f_C(i,j);\quad D_1(i,j)=f_C(i,j+\left[\dfrac{N}{2}\right]); \\ D_2(i,j)=f_C(i+\left[\dfrac{M}{2}\right],j);\quad D_3(i,j)=f_C(i+\left[\dfrac{M}{2}\right],j+\left[\dfrac{N}{2}\right]); \\ where\ 0\le i\le \left[\dfrac{M}{2}\right]-1,\ 0\le j\le \left[\dfrac{N}{2}\right]-1. \end{cases} \quad (2)$$

One level of wavelet decomposition generates one approximated sub-image and three detailed sub-images that contain fine structures with horizontal, vertical, and diagonal orientations. An image is decomposed by wavelet transform into one approximated sub-image (A) and three detailed sub-images (D_1, D_2 and D_3). These four sub-images, each of

which has a size of (*M*/2 x *N*/2) pixels, form the wavelet characteristics. The one-level Haar wavelet decomposition is used to precisely locate the pixels with the textural characteristics. Multi-level wavelet decomposition generates coarser representation of the original image. A large number of decomposition levels will result in the fusion effect for the blemishes and may cause localization deviation of the detected flaw [30]. Figure 3 shows the wavelet transforms among two decomposition levels of a structural texture pattern with area blemishes. Figure 3(a) and 3(b) are the transformed images with the first and second decomposition levels.

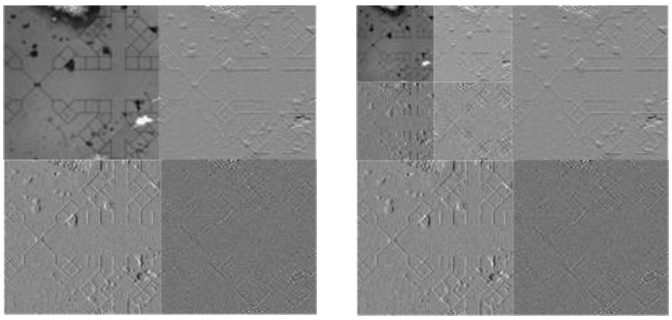

(a) (b)

Figure 3: Decompositions of Fig. 2(b) using Haar wavelet at three decomposition levels: (a) first decomposition level; (b) second decomposition level.

Flat zone filtering

The multi-resolution wavelet technique transforms images into a representation where both spatial and frequency information existing. It is suitable for describing local changes in a homogeneous textured image. For one level of wavelet decomposition, we obtain one approximated sub-image and three detailed sub-images which contain fine structures with horizontal, vertical and diagonal orientations. By properly filtering the approximated sub-image in different decomposition levels for backward wavelet transform, the reconstructed image will remove regular, repetitive texture patterns and enhance only local blemishes. A statistical decision interval can then be used to discriminate between flaw regions and homogeneous regions in the reconstructed image. This converts the difficult flaw detection problem in complicated textured images into a simple interval estimation problem in non-textured images.

Based on the fluctuations of the frequency trend and the properties of the low and high frequency zones, we design a flat zone filter centered at the origin of the 2-D wavelet spectrum to filter out major low frequency components of the spectrum image. An adequate band is first selected for the flat zone filter in the spectrum space. Frequency components within the band of the flat zone filter (low frequencies) are then set to the mean value of frequency, and those outside the filter (medium and high frequencies) are retained. Finally, the inverse wavelet transform is applied to transform the filtered image back to the spatial domain. Choosing a right band based on the degree of frequency changes for the flat zone filtering operation can significantly enhance the area blemishes in the spatial domain. The enhanced effects can be easily observed in the reconstructed images.

Comparing with regular band filtering, the proposed flat zone filtering uses the mean value of overall frequency instead of zero to replace the frequency components within the selected zone area in wavelet frequency domain. The flat zone filtering approach is to reduce the variation between background and texture. The main purpose is to remove the directional background textures which with small changes in grayscales, and reserve the area blemishes which with larger changes in grayscales. We use the concept of statistical decision interval to determine the flat zone area $\bar{x} \pm k\sigma$ and replace all of the frequency components within the region by the frequency mean value $\bar{x}$. This can be written as,

$$\begin{cases} image(i,j) = \bar{x}, \bar{x} - k\sigma < image(i,j) < \bar{x} - k\sigma \\ image(i,j) = image(i,j), otherwise \end{cases} \quad (3)$$

Reverse Wavelet transform

After the proper zone is determined, the frequency filtering operation can accurately specify the non-flaw low frequency regions and set the values of their frequencies at the mean value in the wavelet domain. Then, we can transform the filtered frequency image back to the spatial domain for further flaw separation. In this study, we would like to remove all repeated patterns in the reconstructed image by selecting a proper band in the approximated sub-images for the mean value replacement. Since a structural texture may present high directionality, reconstructing the detailed sub-images with direction emphasis different from that of the regular texture will delete all directional repeated patterns in the original image, and preserve only local blemishes in the reconstructed image. The repetitive, directional patterns will result in an approximately uniform gray level, whereas the local blemishes will yield distinct gray levels in the reconstructed image.

To compare the flaw enhancement effect of filtering in the approximated sub-image, Figure 4 shows the reconstructed images of the two different filtering operations. Figure 4(a) is the result of frequency components replacing by zero and shows most of the repeated patterns are detected as blemishes and some blemishes are missing. Figure 4(b) is the result of frequency components replacing by mean value and shows the directional patterns become approximately uniform in gray level and the flaw regions are significantly enhanced.

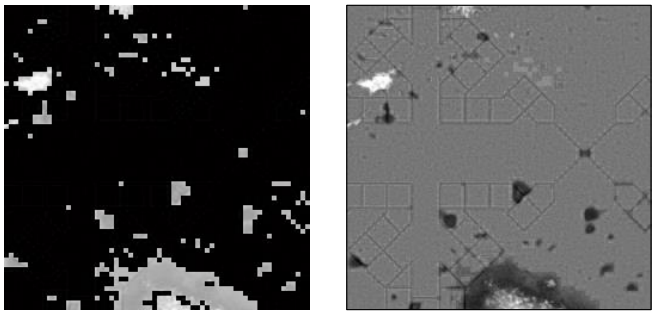

(a) (b)

Figure 4: The reconstructed images with different flat zone filtering values: (a) frequency components replaced by zero; (b) frequency components replaced by mean value.

Flaw separation

The reconstructed image has uniform gray levels for pixels belonging to homogeneous background regions, but it also gives significantly different gray levels for pixels belonging to inhomogeneous flaw areas. The intensity variation in homogeneous regions will be very small, whereas the intensity variation in inhomogeneous areas will be large compared with the entire reconstructed image. Therefore, we can use a statistical method to set up an interval for distinguishing blemishes from repeated patterns in the reconstructed image. The reconstructed image $f'(x, y)$ will be approximately a uniform gray-level image if a non-flaw appearance image is tested. The upper and lower interval limits (T_L, T_U) for intensity variation in the reconstructed image are given by

$$T = \mu_{f'} \pm \ell\, \sigma_{f'} \tag{4}$$

where T is a threshold for segmenting blemishes from background, ℓ is a control parameter, $\mu_{f'}$ and $\sigma_{f'}$ are the mean and standard deviation of the testing reconstructed image of size $M \times M$. The resulting multiple level image $B(x, y)$ for flaw separation is

$$B(x,y) = \begin{cases} 127, & f'(x,y) > T_U \\ 255, & T_L \le f'(x,y) \le T_U \\ 0, & f'(x,y) < T_L. \end{cases} \tag{5}$$

If a gray level value falls within the interval limits (T_L, T_U) then intensity is set to 255 (white) as a background. Otherwise, intensity is set to 0 (black) as a part of dark flaw if a gray level is less than the lower interval limit and intensity is set to 127 (gray) as a part of bright flaw if a gray level is more than the upper interval limit.

If a pixel with the gray level falls within the interval limits, the pixel is classified as a homogeneous element. Otherwise, it is classified as a flaw element. As the flaw size to be inspected are generally very small compared with the entire appearance image, $\mu_{f'}$ and $\sigma_{f'}$ can be computed directly from the reconstructed image of a testing image to accommodate the variation of lighting in the inspection environment. All experimental samples demonstrated in this study are based on the $\mu_{f'}$ and $\sigma_{f'}$ from testing images, and the control constant ℓ is set at different values.

The interval limits are used to distinguish between homogeneous line patterns and blemishes in a filtered reconstructed image. The upper and lower interval limits of gray levels in a reconstructed image are placed at a distance $\ell\sigma_{f'}$ from the mean $\mu_{f'}$. Figure 5 depicts the resulting multiple level images without and with wavelet based flat zone filtering of the reconstructed images, where pixels with gray levels falling outside the interval limits are represented by black and gray intensities (flaw regions), and the ones falling within the limits are represented by white intensity (homogeneous regions). There are many false alarms existing in Fig. 5(a) and most of the area blemishes are correctly detected in Fig. 5(b). This indicates the proposed wavelet based flat zone filtering method has the ability to precisely locate the area blemishes in directional textures. In additions, selecting a proper control parameter results in correctly discriminating blemishes from normal regions but an improper control parameter produces many erroneously detecting normal regions as blemishes. A smaller constant value ℓ gives a tight control and may result in false alarms. A larger constant value ℓ gives a loose control and may generate missing alarms.

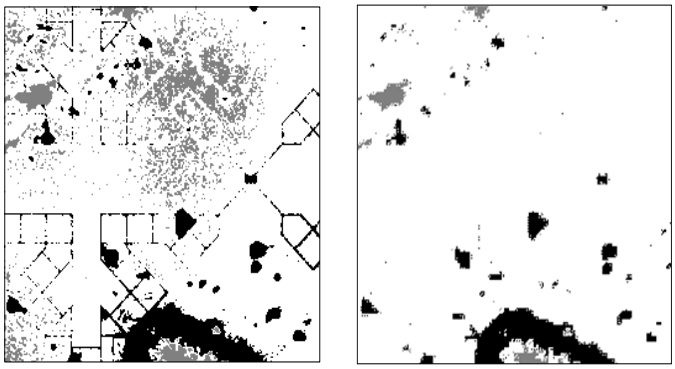

(a) (b)

Figure 5: The resulting multiple level images of flaw detection with and without wavelet flat zone filtering: (a) without wavelet filtering; (b) with wavelet filtering.

A supervised appearance inspection problem is explored in this study. The developed supervised systems are common in machine vision and are appropriate for controlled circumstances in manufacturing. The number of wavelet decomposition levels and the size of flat zone filtering used for image reconstruction are predetermined from a texture model. The impact of number of multi-resolution levels and

sub-image filtering parameters on detection results are empirically evaluated in the following section.

EXPERIMENTAL RESULTS

To evaluate performance of the proposed system, experiments were conducted on real capacitive touch panels provided by a touch panel manufacturing company in Taiwan. All testing samples were randomly selected from the manufacturing process of touch panels. The CTP images (120) with thickness 0.78mm, of which 52 have no blemishes and 68 have various area blemishes, were tested in our experiments. Each image of the appearance has a size of 256 x 256 pixels and a gray level of 8 bits. The area flaw detection algorithm is edited and executed on the R2009b version of the MatLab software on a personal computer (CPU i5-3230M 2.6 GHz and 4GB RAM).

To further quantitatively verify the performance of the proposed method, we compare the results of our experiments against those provided by professional inspectors. Three objective indices: correct judgment (CR) and erroneous judgments (α and β) were evaluated for the performance of the area flaw detection methods. Statistical type I error α suggests the probability of producing false alarms, i.e. detecting normal regions as blemishes. The area of normal region detected as blemishes is divided by the area of actual normal region to obtain type I error. Statistical type II error β implies the probability of producing missing alarms, which fail to alarm real blemishes. The area of undetected blemishes is divided by the area of actual blemishes to obtain type II error. The higher the performance evaluation indices: (1-α), (1-β), and correct classification rate, the more accurate the detection results. The correct classification rate (CR) is defined as

$$CR = (N_{(1-\alpha)} + N_{(1-\beta)}) / N_{total} \times 100\% \quad (6)$$

where $N_{(1-\alpha)}$ is the pixel number of normal textures detected as normal areas, $N_{(1-\beta)}$ is the pixel number of real blemishes detected as defective regions, and N_{total} is the total pixel number of a testing image.

Selection of the appropriate decomposition level in wavelet domain

Wavelet transform decomposition of a textured image in its proper level will effectively highlight the local blemishes in the homogeneous appearance. To evaluate the impact of varying number of decomposition levels on the reconstruction result, Figures 6(a) to 6(d) present the reconstructed images from decomposition levels 1, 2, 3, and 4, respectively. All these images are individually reconstructed from a filtered approximated sub-image and three corresponding detailed sub-images with the Haar wavelet. Both Figures 6(a) and 6(b) reveal that too small the number of decomposition levels (such as 1 and 2) cannot sufficiently separate blemishes from the repetitive texture patterns and causes many false alarms. However, too large the number of decomposition levels (such as 4 in Figure 6(d)) produces the fusion effect of the blemishes and results in erroneous detection of missing alarms. The number of decomposition level 3 (Figure 6(c)) is more appropriate to enhance blemishes in the reconstructed image. Our experiments on a variety of textures images have confirmed that WAVELET decomposition level 3 is generally sufficient for this area flaw detection application.

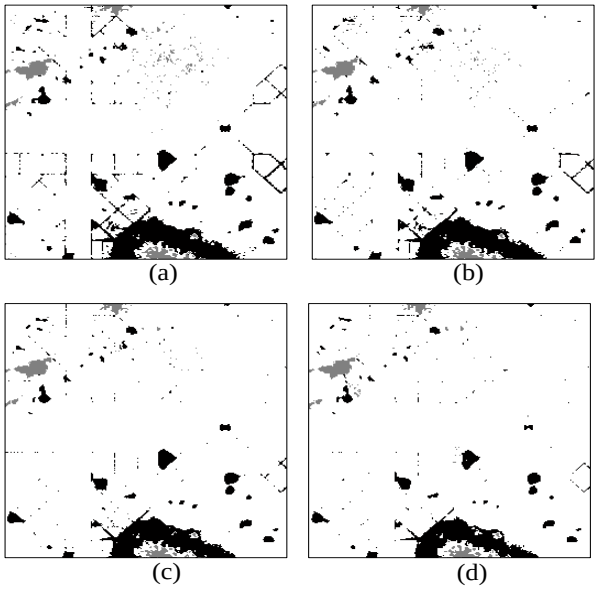

Figure 6: Resulting images of flaw detection at four wavelet decomposition levels: (a) first decomposition level; (b) second decomposition level; (c) third decomposition level; (d) fourth decomposition level.

Selection of flat zone size for filtering in wavelet domain

As the decision threshold value changes, so do its false alarm rate (α) and detection rate (1-β), both of which are used to describe the performance of a test according to hypothesis testing theory [31]. When various decision thresholds are used, their pairs of false alarm rates and detection rates are plotted as points on a Receiver Operating Characteristic (ROC) curve. The upper-left corner of a ROC curve indicates a perfect result with 100% detection rate and a 0% false alarm rate. The more the ROC curve approaches the upper-left corner, the better the test performs. In industrial practice, a more than 90% detection rate and a less than 10% false alarm rate are a good rule of thumb for performance evaluation of a vision system.

High-energy frequency components associated with periodical line patterns may appear around the primary zones in the wavelet domain image. To significantly filter out all

homogeneous line patterns and completely retain the area blemishes in the spatial domain image, the frequency components on the primary zones must be replaced by the mean value of the frequency components from the wavelet domain image. The filtering width determines the regions of the band neighborhoods will be filtered for high-energy frequency components. Figure 7 demonstrates the ROC curve of the proposed method with different flat zone sizes of k values, 0.8, 1.0, 1.2, 1.4, 1.6, respectively. It shows the flaw detection performance of the proposed method with k value of 1.2 is better than those of the other k values. The flat zone filtering method with larger k value not only removes homogeneous line patterns but also local blemishes in the reconstructed image and result in ignoring small blemishes. Accordingly, an appropriate flat zone size, with its ROC curve closest to the upper-left corner, outperforms the other sizes. This implies that the more accurate regions of band neighborhoods are filtered, the better the flaw detection results will have.

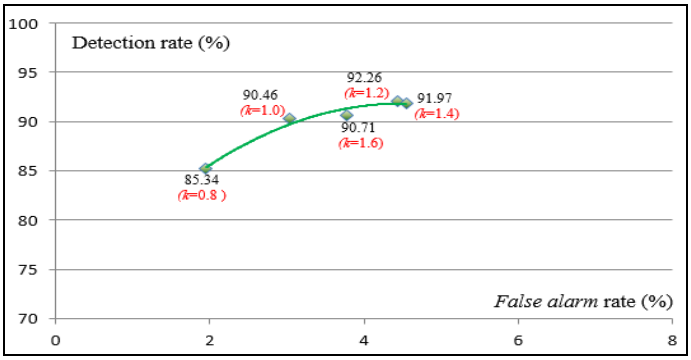

Figure 7: ROC plot of different zone sizes for wavelet filtering.

Comparisons of flaw detection methods

To demonstrate the flaw detection results, Figure 8 lists partial results of detecting area blemishes by the Otsu method [10], the Iterative method [32], the multiple level method (two threshold values in spatial domain without frequency filtering), and the proposed method, individually. The three spatial domain techniques, the Iterative, Otsu, and multiple level methods, make lots of false alarms on area flaw detection. The frequency domain technique, the proposed method, detects most of the area blemishes and makes less erroneous judgments. Therefore, the frequency domain approach outperforms the spatial domain techniques in the area flaw detection of the touch panels.

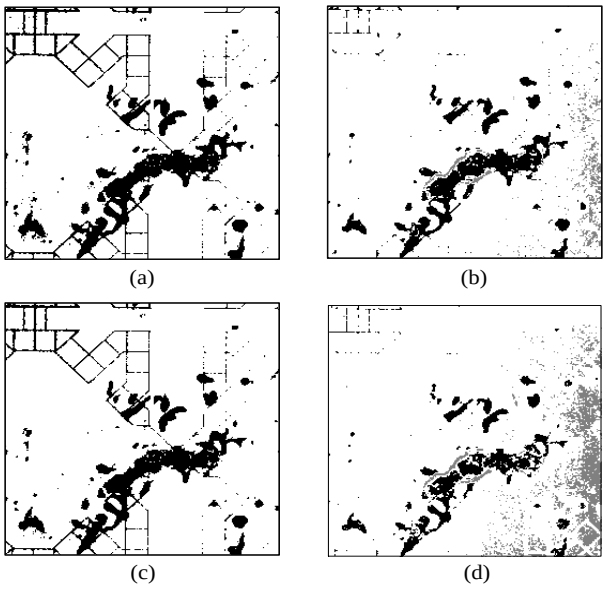

Figure 8: Partial detection results of (a) Iterative, (b) Otsu, (c) multiple level, and (d) the proposed methods.

To compare the performance of the area flaw detection, the following description summarizes the detection results of our experiments. Three spatial domain approaches and one frequency domain technique are evaluated against the results by professional inspectors. The average flaw detection rates (1-β) of all testing samples by the four methods are, respectively, 78.88% (Iterative method), 80.27% (Otsu method), 86.48% (multiple level method), and 90.68% (proposed method). However, the three spatial domain methods have significantly higher false alarm rates (α), 21.51% (Iterative method), 27.72% (Otsu method), and 12.64% (multiple level method). On the contrary, the proposed approach has rather lower false alarm rate, 5.53%. In addition, the proposed method has higher correct classification rates (CR) than do the other methods applied to area flaw detection of touch panel images. The average computation time for processing an image of 256 x 256 pixels is as follows: 0.04 seconds by the Otsu method, 0.06 seconds by the Iterative method, 0.14 seconds by the multiple level method, and 0.16 seconds by the proposed method. Hence, the proposed method can overcomes the difficulties of detecting area blemishes on touch panels and excels in its ability of correctly discriminating area blemishes from normal regions.

CONCLUSIONS

This study presents a quality system based on wavelet transform filtering for automatic inspection of area blemishes in directional textures of touch panels. The repeated line patterns of four directional textures in the spatial domain image can be easily reduced by detecting the band region of an approximated sub-image of a decomposed image in wavelet domain, setting them to mean value of frequency components by the flat zone filter, and transforming back to a

spatial domain image. In the filtered reconstructed image of a textured surface, the periodic line regions in the original image will have an approximately uniform gray level, whereas the defective regions will be clearly retained. A statistical interval is therefore estimated to set up the control limits for discriminating among dark blemishes, bright blemishes, and homogeneous line pattern background. Thus, the intricate area blemishes can be precisely identified by the proposed system. Experimental results show that the proposed method achieves a high 90.68% probability of correctly discriminating area blemishes from normal regions and a low 5.53% probability of erroneously detecting normal regions as blemishes on structural textured appearances of touch panels.

ACKNOWLEDGEMENTS

The authors thank the Ministry of Science and Technology, Taiwan (R.O.C.), for the financial support through the Grant NSC 101-2221-E-324-007-MY2.

REFERENCES

[1] Chiu, Y. P., Lo, Y. C., and Lin, H. D., 2017, "Hough transform based approach for surface distortion flaw detection on transparent glass," International Journal of Applied Engineering Research, 12(19), pp. 8150-8159.

[2] Mananga, E. S., El Fakhri, G., Schaefferkoetter, J., Bonab, A. A., and Ouyang, J., 2014, "Myocardial defect detection using PET-CT: phantom studies," PLoS ONE, 9(2): e88200.

[3] Chiu, Y. P., and Lin, H. D., 2013, "An innovative blemish detection system for curved LED lenses," Expert Systems with Applications, 40(2), pp. 471-479.

[4] Lin, H. D., Chiu, Y. P., and Lin, W. T., 2013, "An innovative approach for detection of slight surface variations on capacitor chips," International Journal of Innovative Computing Information and Control, 9(5), pp. 1835-1850.

[5] Xie, X. 2008, "A review of recent advances in surface defect detection using texture analysis Techniques," Electronic Letters on Computer Vision and Image Analysis, 7(3), pp. 1-22.

[6] Kuo, C. J., and Su, T., 2003, "Gray relational analysis for recognizing fabric defects," Textile Research Journal, 73(5), pp. 461–465.

[7] Yoon, Y. G., Lee, S. L., Chung, C. W., and Kim, S. H., 2008, "An effective defect inspection system for polarized film images using image segmentation and template matching techniques," Computers & Industrial Engineering, 55, pp. 567-583.

[8] Yuan, T, and Kuo, W., 2008, "Spatial defect pattern recognition on semiconductor wafers using model-based clustering and Bayesian inference," European Journal of Operational Research, 190, pp. 228-240.

[9] Sezgin, M., and Sankur, B., 2004, "Survey over image thresholding techniques and quantitative performance evaluation," Journal of Electronic Imaging, 13 (1), pp. 146-156.

[10] Otsu, N., 1979, "A threshold selection method from gray level histogram," IEEE Transactions on Systems, Man and Cybernetics, 9, pp. 62-66.

[11] Ng, H. F., 2006, "Automatic thresholding for defect detection," Pattern Recognition Letters, 27, pp. 1644-1649.

[12] Navarro, P., Iborra, A., Fernández, C., Sánchez, P., and Suardíaz, J., 2010, "A sensor system for detection of hull surface defects," Sensors, 10, pp. 7067-7081.

[13] Gonzalez, R. C., 2008, Woods RE. Digital Image Processing, 3rd Ed., Prentice Hall, New Jersey, USA.

[14] Nasira, G. M., and Banumathi, P., 2013, "Fourier transform and image processing in automated fabric defect inspection system," International Journal of Computational Intelligence and Informatics, 3(1), pp. 61-64.

[15] Tsai, D. M., and Hsiao, B., 2001, "Automatic surface inspection using wavelet reconstruction," Pattern Recognition, 34, pp. 1285-1305.

[16] Lin, H. D., 2007, "Automated visual inspection of ripple defects using wavelet characteristic based multivariate statistical approach," Image and Vision Computing, 25, pp. 1785-1801.

[17] Li, T. S., 2009, "Applying wavelets transform and support vector machine for copper clad laminate defects classification," Computers & Industrial Engineering, 56, pp. 1154-1168.

[18] Chang, H. F., 2012, "Design and implementation of real-time fabric defect detection system," Advances in information Sciences and Service Sciences, 4(21), pp. 23-30.

[19] Lin, H. D., and Chiu, S. W., 2011, "Flaw detection of domed surfaces in LED packages by machine vision system," Expert Systems with Applications, 38, pp. 15208-15216.

[20] Ngan, H. Y. T., Pang, G. K. H., and Yung, N. H. C., 2011, "Automated fabric defect detection - A review," Image and Vision Computing, 29, pp. 442-458.

[21] Timm, F, and Barth, E., 2012, "Novelty detection for the inspection of light-emitting diodes," Expert

Systems with Applications, 39, pp. 3413-3422.

[22] Lu, C. J., and Tsai, D. M., 2008, "Independent component analysis-based defect detection in patterned liquid crystal display surfaces," Image and Vision Computing, 26, pp. 955-970.

[23] Perng, D. B., and Chen, S. H., 2010, "Automatic surface inspection for directional textures using nonnegative matrix factorization," International Journal of Advanced Manufacturing Technology, 48, pp. 671-689.

[24] Chen, Y. C., Yu, J. H., Xie, M. C., and Shiou, F. J., 2011, "Automated optical inspection system for analogical resistance type touch panel," International Journal of the Physical Sciences, 6 (22), pp. 5141-5152.

[25] Lin, H. D., and Tsai, H. H., 2012, "Automated quality inspection of surface defects on touch panels," Journal of the Chinese Institute of Industrial Engineers, 29(5), pp. 291-302.

[26] Arivazhagan, S., and Ganesan, L., 2003, "Texture segmentation using wavelet transform," Pattern Recognition Letters, 24, pp. 3197-3203.

[27] Bashar, M. K., Matsumoto, T., and Ohnishi, N., 2003, "Wavelet transform-based locally orderless images for texture segmentation," Pattern Recognition Letters, 24, pp. 2633-2650.

[28] Kim, S. C., and Kang, T. J., 2007, "Texture classification and segmentation using wavelet packet frame and Gaussian mixture model," Pattern Recognition, 40, pp. 1207-1221.

[29] Li, W. C., and Tsai, D. M., 2012, "Wavelet-based defect detection in solar wafer images with inhomogeneous texture," Pattern Recognition, 45, pp. 742-756.

[30] Tsai, D. M., and Chiang, C. H., 2003, "Automated band selection for wavelet reconstruction in the application of defect detection," Image and Vision Computing, 21, pp. 413-431.

[31] Duda, R. O., Hart, P. E., and Stork, D. G., 2000, Pattern Classification, 2th Ed., John Wiley & Sons, New Jersey, USA.

[32] Jain, R, Kasturi, R, and Schunck, B. G., 1995, Machine Vision, International Editions, McGraw Hill, New York, USA.